A Near-Real-Time Automatic Orbit Determination System for COSMIC and Its Follow-On Satellite Mission: Analysis of Orbit and Clock Errors on Radio Occultation

Yi-Shan Li, Cheinway Hwang, Tzu-Pang Tseng, Cheng-Yung Huang, and Heike Bock

Abstract—The COSMIC-2 mission is a follow-on mission of the Constellation Observing System for Meteorology, Ionosphere, and Climate (COSMIC) with an upgraded payload for improved radio occultation (RO) applications. The objective of this paper is to develop a near-real-time (NRT) orbit determination system, called NRT National Chiao Tung University (NCTU) system, to support COSMIC-2 in atmospheric applications and verify the orbit product of COSMIC. The system is capable of automatic determinations of the NRT GPS clocks and LEO orbit and clock. To assess the NRT (NCTU) system, we use eight days of COSMIC data (March 24–31, 2011), which contain a total of 331 GPS observation sessions and 12 393 RO observable files. The parallel scheduling for independent GPS and LEO estimations and automatic time matching improves the computational efficiency by 64% compared to the sequential scheduling. Orbit difference analyses suggest a 10-cm accuracy for the COSMIC orbits from the NRT (NCTU) system, and it is consistent as the NRT University Corporation for Atmospheric Research (UCAR) system. The mean velocity accuracy from the NRT orbits of COSMIC is 0.168 mm/s, corresponding to an error of about 0.051 μrad in the bending angle. The rms differences in the NRT COSMIC clock and in GPS clocks between the NRT (NCTU) and the postprocessing products are 3.742 and 1.427 ns. The GPS clocks determined from a partial ground GPS network [from NRT (NCTU)] and a full one [from NRT (UCAR)] result in mean rms frequency stabilities of 6.1E-12 and 2.7E-12, respectively, corresponding to range fluctuations of 5.5 and 2.4 cm and bending angle errors of 3.75 and 1.66 μrad.

Index Terms—Constellation Observing System for Meteorology, Ionosphere, and Climate (COSMIC), COSMIC-2, GPS, orbit determination (OD), radio occultation (RO).

I. INTRODUCTION

THE COSMIC-2 mission [1] is a follow-on mission to continue the Constellation Observing System for Meteo-

rology, Ionosphere, and Climate (COSMIC) mission in radio occultation (RO) applications. The COSMIC and COSMIC-2 missions are named FORMOSAT-3 and FORMOSAT-7 by the National Space Organization (NSPO) of Taiwan. COSMIC is one of the GPS RO satellite missions that have delivered promising RO data and products to the scientific community [2], [3]. Sample publications using COSMIC data can be found in the COSMIC special issue of the IEEE Transactions of Geoscience and Remote Sensing, Vol. 46, No.11, 2008. Six of the 12 COSMIC-2 satellites (first launch) will be deployed in 2016 at inclination angles ranging from 24° to 28.5° and altitudes from 520 to 550 km. In the second launch in 2018, the remaining satellites will be deployed at an inclination angle of 72°, with altitudes ranging from 720 to 750 km. COSMIC-2 will provide more than 8000 RO soundings per day when all satellites are in the operational phase (see [1] and http://www.nspo.org.tw/2008e/projects/project7). Each of the COSMIC-2 satellites will be equipped with an advanced Global Navigation Satellite System (GNSS) receiver, called the TriG receiver, to receive high-quality GNSS signals from GPS, Galileo, and GLObal NAvigation Satellite System (GLONASS) for orbit determination (OD) and RO applications [4], [5]. A retroreflector for satellite laser ranging (SLR) may be installed on some of the COSMIC-2 satellites to provide SLR measurements to validate and enhance the GNSS-derived orbits of the COSMIC-2 satellites [6], [7]. With the multiple GNSS satellite signals, improved payload performance, a global GNSS tracking network, and the SLR enhancement for OD and validation, COSMIC-2 is expected to deliver an improved product over COSMIC for atmospheric and geodetic applications.

The first step in the retrieval of physical properties of the atmosphere from RO data is to determine the atmospheric excess phase in the phase measurements of GPS (or GNSS for multiple systems). Excess phase is due to the delay and bending of GPS signals in the Earth's atmosphere and ionosphere [8], [9]. To generate the excess phase, the orbits of the GPS and low-Earth-orbiting satellites must be given [10]. Currently, for the operational use of COSMIC RO data, the near real time (NRT) orbits and clocks of the COSMIC satellites are provided by the University Corporation for Atmospheric Research (UCAR). For a numerical assimilation of RO data into a weather forecast model (particularly in the case of extreme weathers

such as typhoon and cyclone), the excess phase must be determined in real time for the RO data to be effective in model improvement [11].

The objective of this paper is twofold. The first is to develop an NRT OD system to support the COSMIC-2 mission and to verify the system that is currently in use in the NRT applications of COSMIC data. By executing existing well-established computer modules, the OD system will determine the following: 1) NRT high-rate clock corrections of GPS satellites; 2) NRT precise orbits of COSMIC satellites (at decimeter level); and 3) NRT clock corrections of COSMIC satellites. For the reason given in Section III, the NRT determination of GPS satellites will not be included in the OD system. The verification will be made using the COSMIC data and by comparison with the results from the NRT (UCAR) system used in the COSMIC Data Analysis and Archival Center (CDAAC) of UCAR. The NRT (UCAR) system is also used in the Taiwan Analysis Center for COSMIC (TACC) of the Central Weather Bureau, Taiwan [1], [12]. The second objective is to see how the product from the NRT National Chiao Tung University (NCTU) system (GPS clock corrections and the orbit and clock corrections of COSMIC) affects excess phase, excess Doppler shift, and bending angle in RO events, with case studies using the COSMIC data. For convenience, the six COSMIC satellites will be named FM1–FM6 in this paper.

II. AUTOMATIC SYSTEM FOR NRT DETERMINATIONS OF SATELLITE ORBIT AND CLOCK

Currently, up to eight International GNSS Service (IGS) analysis centers provide daily ultrarapid, rapid, and final GPS products, such as precise orbit and clock solutions (http://igscb. jpl.nasa.gov/igscb/resource/pubs/UsingIGSProductsVer21.pdf). Among others, they are the Center for Orbit Determination in Europe (CODE), Natural Resources Canada (NRCan), European Space Agency (ESA), GeoForschungsZentrum Potsdam (GFZ), Jet Propulsion Laboratory (JPL), Massachusetts Institute of Technology, National Geodetic Survey, and Scripps Institute of Oceanography [13], [14]. Recently, some institutes have developed a system for the estimations of NRT GPS orbit and clock products. For example, the IGS Real-Time Pilot Project is to improve the existing real-time infrastructure of IGS and to provide an official real-time service [15], [16]. The project is mainly supported by Bundesamt für Kartographieund Geodäsie, Centre National d'Etudes Spatiales, Czech Technical University, Deutsches Zentrum für Luft-und Raumfahrt, European Space Operations Center (ESOC), Geo++ (Gesellschaft für satellitengestützte und navigatorische Technologien mbH), GMV Aerospace and Defence, NRCan, and Wuhan Technical University. Under this project, the IGS real-time analysis centers determine GNSS clock corrections using the IGS ultrarapid orbits and real-time data from over 100 stations in the IGS network. The final real-time product is a combination of the real-time products from the participating centers [17]–[19].

The qualities of the NRT GPS clock and orbit are crucial for the NRT precise OD (POD) of the low Earth orbiter (LEO) satellite. For a convenient and independent processing of future
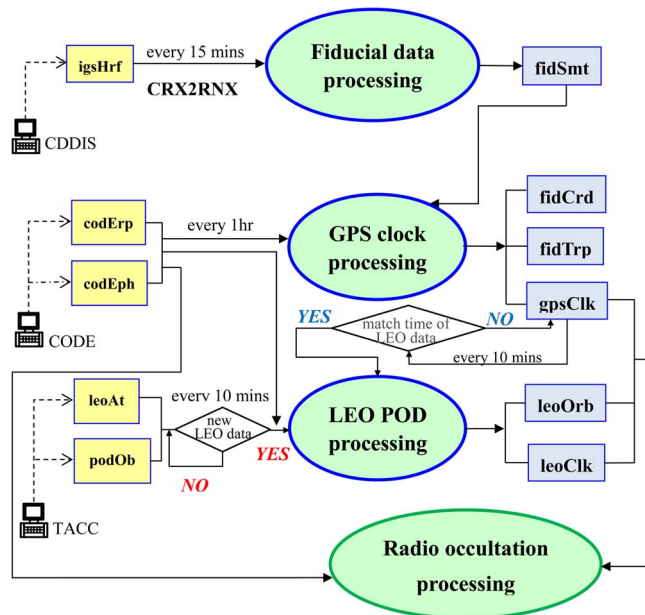

Fig. 1. Flowchart of the automatic NRT OD system under a Linux/PC cluster.

COSMIC-2 OD, in this paper, we develop an automatic system under a Linux environment in a PC cluster to determine the following: 1) NRT high-rate GPS clocks (30 s) and 2) NRT orbit and clock of COSMIC satellites. Here, clock means clock correction estimate, either for the transmitter clock on board a GPS satellite or for the receiver clock on board a COSMIC (or COSMIC-2) satellite. Hereafter, the system is named the NRT (NCTU) system, in comparison to the NRT (UCAR) system used in UCAR. A low-altitude satellite is sometimes called a LEO in the RO literature. The system is automatic in that a job scheduler using Perl programs and shell scripts executes designated jobs automatically. The GPS part of the data processing in the system is handled by the Bernese Processing Engine (BPE), with the core program being the Bernese GPS Software Version 5.0 [20]. BPE is widely used in the automatic processing of large-volume GPS data. For example, since 1995, CDAAC and CODE use BPE for the routine processing of ground-based GPS data and, later, for the POD of space (LEO)-based GPS data [21]. Another sample user of BPE is the Geographical Survey Institute of Japan, whose GPS network data provide major displacement measurements associated with the March 11, 2011 earthquake [22]. The Open Portable Batch System (OpenPBS), a job and computer system resource management package, is used to arrange the sequence of job execution. With BPE and OpenPBS, the NRT (NCTU) system can simultaneously process GPS data from different LEO receivers and from a ground network.

The NRT (NCTU) system contains three parts: the fiducial data processing, GPS clock processing, and LEO POD processing (see Fig. 1). The fiducial data processing is responsible for downloading, combining, and smoothing the GPS high-rate (1-Hz) tracking data. The GPS clock processing determines the following: 1) the zenith tropospheric delays (ZTDs) at selected GPS ground stations and 2) the 30-s GPS clocks from the smoothed GPS data. The LEO POD processing takes care of the determination of the orbit and clock of LEOs. The product
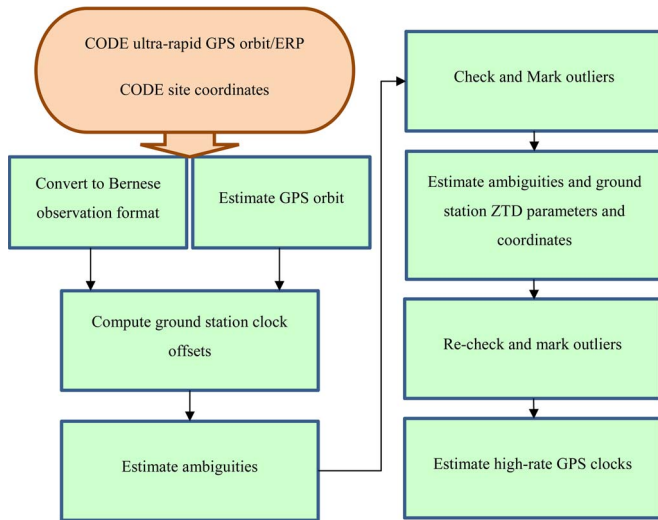
Fig. 2. Processing flow of NRT high-rate GPS clock determination using zero-differenced observations.
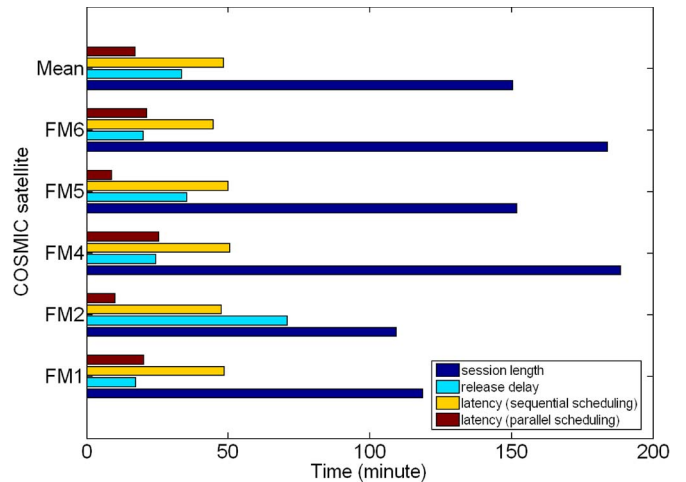

Fig. 3. Mean times for GPS session length, release delay, and latency of COSMIC orbit processing using sequential and parallel schedulings over DOY 83–90, 2011.

from this system is used to compute the excess phase and excess Doppler shift, which, in turn, are used to retrieve atmospheric parameters (see Section V). Fig. 1 shows the components of the NRT (NCTU) system. The rectangular boxes contain the input/output (IO) data, with the yellow-shaded ones representing input and the light sky blue-shaded ones representing output. The blue ellipses contain the data processing components. The time along an arrow shows the time associated with one IO. The NRT (NCTU) system processes ground GPS data every 15 min and determines GPS clocks every 1 h. Every 10 min, the system detects newly arriving data downlinked from LEOs (the YES/NO in red). If such data are detected, the system will download the data and then determine the LEO orbit and clock. The input and output data in Fig. 1 are listed as follows:

1) Input:
   a) igsHrf: 1-Hz GPS data at ground stations from the Crustal Dynamics Data Information System (CDDIS);
   b) codErp and codEph: ultrarapid Earth rotation parameters and GPS orbits from CODE;
   c) leoAtt and podObs: NRT attitudes and GPS observations of LEOs from TACC.
2) Output:
   a) fidSmt: smoothed ground GPS data at 30-s intervals;
   b) fidCrd and fidTrp: station coordinates and ZTD;
   c) gpsClk: high-rate GPS clocks at 30-s intervals;
   d) leoOrb and leoClk: orbit and clock of LEOs.

Fig. 2 shows the procedure to estimate the high-rate GPS clocks needed for direct RO applications and for determining the orbit and clock of LEOs. With the station coordinates and tropospheric information fixed, the procedure uses epoch-differenced phase observations and the GPS ultrarapid orbits to solve for high-rate GPS clocks [23]. In addition, the procedure for solving the LEO orbit and clock in the NRT case equals the procedure in the postprocessing (PP) case, and it is described in detail in [24] and [25]. The major difference is that the NRT GPS clocks and ultrarapid GPS orbits are used in the NRT case, while the final GPS clocks and orbits are used in the PP case.

For COSMIC, the current mean latency from receiving GPS data to releasing RO products is 75 min. For COSMIC-2, the latency is expected to be 45 min. Because COSMIC-2 requires a smaller latency than COSMIC and the number of LEOs in COSMIC-2 doubles that of COSMIC, an efficient processing algorithm for COSMIC-2 must be developed. To find an efficient processing algorithm for COSMIC-2, we experiment with two schedulings for estimating high-rate GPS clocks. In the first scheduling, called sequential scheduling, the system will perform individual GPS clock estimations for all satellites of COSMIC according to individual GPS observations. It results in redundant computations of GPS clocks. With 12 satellites in COSMIC-2, the redundant computation of GPS clocks in the sequential scheduling is even larger. In the second scheduling, called parallel scheduling, the estimation of GPS clocks is independent (every hour routine in this paper) from and parallel with the estimation of the LEO orbit, and the OD system will automatically match the time of a LEO orbit arc with the times of the available GPS clocks to compute the LEO orbit. The advantage of the parallel scheduling is its independent determination of GPS clocks and its efficiency, particularly when multiple LEO arcs need the same GPS clocks for OD computations. Fig. 1 also shows the parallel scheduling. Every 10 min, the system compares the times of the estimated GPS clocks with the times of LEO data sessions to extract the needed GPS clocks for determining the orbit and clock of LEOs (the YES/NO in blue). Fig. 3 shows the mean session lengths of GPS data on five COSMIC satellites, the release delay, and the latencies based on the sequential and parallel schedulings over day of year (DOY) 83–90, 2011. The "session length" is defined as the period between the first and the last epoch of the GPS observations. The "release delay" is defined as the period between the time tag of the released file and the last epoch of the GPS observations. The "latency" is defined as the difference between the epoch of the orbit generation and the last epoch of the GPS observations. The overall mean session length and data release delay (see top charts in Fig. 3) are 150 and 26 min, respectively. When using the sequential scheduling,

the mean LEO processing time (mainly for the LEO orbit and clock) is 48.0 min, compared to only 17.2 min with the parallel scheduling. In this example, the use of the parallel scheduling improves the LEO OD by 64%.

III. DETERMINATION AND ASSESSMENT OF NRT HIGH-RATE GPS CLOCKS

The precise GPS clocks are a critical factor in the NRT OD and RO applications (see Section V). For example, a 0.1-ns clock error will cause a 3-cm error in range, which affects the orbit accuracy by about the same amount. The final and rapid GPS products are not usable for an NRT application because they cannot be obtained in real time. The ultrarapid GPS product from CODE, including orbits, clocks (from the GPS broadcast clocks), and Earth rotation parameters, is updated every 6 h with a latency of 3 h. The ultrarapid GPS orbits and clocks cover a period of 48 h, with the first 24-h product from real observations and the remaining part containing predicted orbit and clock information. The ultrarapid GPS product can be obtained from the ftp site of CODE (ftp://ftp.unibe.ch/aiub/CODE).

The accuracies of GPS orbits and clocks govern the accuracy of the NRT orbit of a LEO. According to Wickert et al. [26] and Michalak and Konig [27], the use of the ultrarapid orbit is sufficient for NRT OD (at the required accuracy level), and updating the CODE ultrarapid orbit more often is not necessary for an NRT OD. Therefore, the NCTU OD system estimates only real-time high-rate (30-s) GPS clocks and use ultrarapid GPS orbits from CODE without estimating GPS orbits. The accuracy of the CODE ultrarapid orbits is about 10 cm and is sufficient for NRT LEO OD processing. In general, the quality of the predicted GPS clocks decreases with the length of prediction [28]. In order to improve the quality of the NRT OD, we determine the NRT high-rate GPS clocks at 30-s intervals in this paper by using the efficient high-rate clock interpolation method in [23] and [28].

For the computational efficiency, we estimated only the high-rate clocks of GPS at 30-s intervals. In fact, the use of the 30-s clocks will affect NRT RO results slightly as compared to the use of 1-s clocks. This is demonstrated by Schreiner et al. [29], who compared the bending angle and refractivity estimated with 30-s GPS clocks (SD-30s) and 1-s GPS clocks (SD-1s) using single differencing. By the PP procedure, the noises of the neutral atmospheric bending angle for cases of SD-30s and SD-1s GPS clocks are 1.52E-6 and 1.47E-6, respectively. Indeed, the SD-1s case can reduce noise over the SD-30s case by about 3%. Schreiner et al. [29] also show that the standard deviation of the difference between the GPS RO and high-resolution European Centre for Medium-Range Weather Forecasts (ECMWF) refractivity profiles at an altitude of 30 km is 0.60% for SD-1s GPS clocks and 0.68% for SD-30s GPS clocks. The use of SD-1s can reduce the difference of refractivity, but it would linearly extend the processing time of the clock interpolation [23], [28]. If our NRT OD system estimates the 1-s GPS clocks, the processing will take at least 20 min longer. That is inefficient for the NRT application.

TABLE I
RMS AND MEAN DIFFERENCES IN GPS CLOCK (IN NANOSECONDS) BETWEEN TWO SOLUTIONS

Case	RMS	Mean
[1]NRT (NCTU) – PP (CODE)	1.427	-0.292
[1]NRT (UCAR) – PP (CODE)	1.332	-0.515
[1]NRT (NCTU) – NRT (UCAR)	1.939	-0.202
[2]NRT (NCTU) – NRT (ESA)	1.559	-0.551

[1] data over DOY 83-90, 2011
[2] data over DOY 345-347, 2011

The most critical limitation for GPS high-rate clock estimation is the real-time availability of GPS data from the global network. To estimate the GPS clocks, CDAAC and TACC use GPS data from a global network of GPS tracking stations operated by IGS, NRCan, European Organization for the Exploitation of Meteorological Satellites (EUMETSAT), and CDAAC (private communication, TACC, Taiwan). The fiducial databases belong to the institutions collaborating with CDAAC and TACC under agreements with them. Fig. 4(a) shows the distribution of the fiducial stations from the four different tracking databases at TACC. IGS, NRCan, EUMETSAT, and CDDAC provide about 40, 10, 35, and 4 GPS stations, respectively. At TACC, the minimum number of stations to estimate the station ZTDs and GPS clocks is 37. However, the actual number of stations is larger than 37 and can be up to 85 depending on how many NRT fiducial data the TACC receives (private communication, TACC, Taiwan).

Because our team does not have agreements with NRCan, EUMETSAT, and CDDAC, in this paper, we validated our NRT OD system using only the publicly available GPS tracking data of IGS from CDDIS (ftp://cddis.gsfc.nasa.gov/highrate). The data were sampled at 1 Hz and updated every 15 min. In order to minimize the latency and maximize the amount of ground tracking data, the procedure in this paper was executed at some selected (optimal) times, rather randomly. The number of the GPS stations that were actually used depends on the latency of the tracking stations. Over the selected days, the average number of the available GPS stations is about 50. For example, Fig. 4(b) shows the distribution of the available GPS stations for session C (UTC = 2 ∼ 3 h) of DOY 86. Our system will estimate the high-rate GPS clocks automatically every hour by the automatic procedure without any intervention. Given the observation time of COSMIC, our system will select the corresponding GPS clock estimates at the same time.

For quality assessment, we compared the GPS clocks estimated in this paper with those from the real-time UCAR product, the final CODE product, and real-time ESA product. The comparison with UCAR and CODE is over DOY 83–90 (March 24–31), 2011, and the comparison with ESA is over DOY 345–347 (December 11–13), 2011. The NRT (ESA) GPS clocks at 30-s sampling intervals are estimated by the NAvigation Package for Earth Observation Satellites
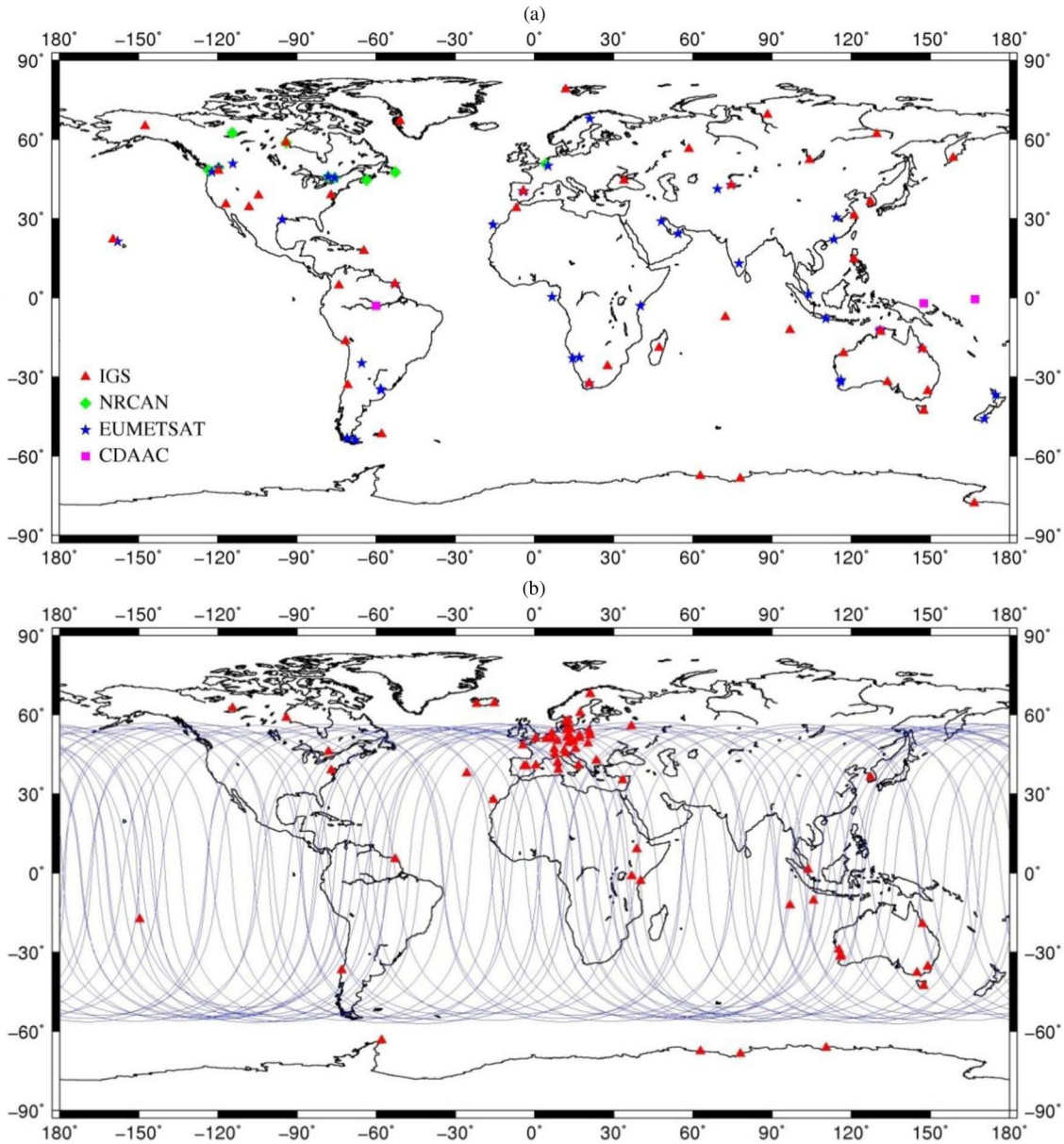
Fig. 4.　Distributions of the ground GPS stations used by (a) TACC and (b) NCTU automatic OD (for experiment in this paper).

(NAPEOS) software in the ESOC of ESA [30]. The final CODE solution is regarded as the true solution of the GPS clocks. Table I summarizes the rms and the mean differences in four cases of comparison. The mean differences among these products (NCTU, UCAR, CODE, and ESA) are consistent at the subnanosecond level. Such differences are partly attributed to different clock references because different products use different clock references. In addition, the differences between the NCTU and UCAR/ESA GPS solutions (rows 3 and 4 in Table I) are larger than those from the other two cases. This is due to the fact that NCTU, UCAR, and ESA solutions are produced in real time and do not use the final GPS orbits and Earth rotation parameters as in the CODE solution. Both the rms and mean (in absolute value) in the NCTU-CODE case are close to those in the UCAR-CODE case (at the 0.1-ns level), suggesting that the performance of our real-time GPS clock estimation (this paper) is consistent with that of UCAR.

However, the fact that the rms and mean from NCTU are larger than those from UCAR and ESA highlights the importance of using more ground stations for the GPS clock estimation. In the NCTU solution, only a limited number of ground stations are used, leading to a less favorable network geometry compared to the geometry associated with UCAR. Despite the degraded geometry in the NCTU solution, the GPS clock estimation already matches the NRT (UCAR) solution to 0.1 ns.

Fig. 5 shows the rms and mean differences as a function of GPS satellites in the four cases. The comparison of NCTU-CODE agrees well with that of NCTU-ESA. The differences in rms and mean values with respect to GPS satellite between NCTU-CODE and NCTU-ESA are lower than 1 ns, except for satellites G19, G22, and G30 (satellite G24 is not available over DOY 345–347, 2011). Satellite G5 has the largest rms and mean differences in all cases, and the mean differences in the cases of NCTU-CODE/NCTU-ESA and UCAR-CODE have opposite
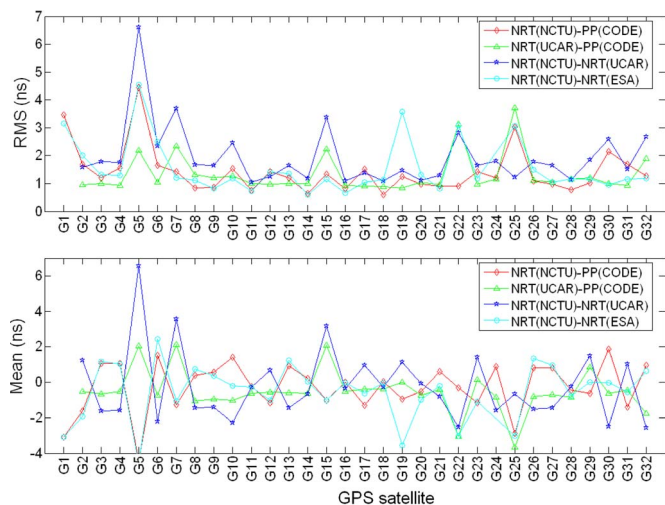
Fig. 5.　(Top) RMS and mean differences in GPS clock (in nanoseconds) between two solutions with respect to GPS satellite. The solutions of NRT (NCTU)-PP (CODE), NRT (UCAR)-PP (CODE), and NRT (NCTU)-NRT (UCAR) are over DOY 83–90, 2011, and the solution of NRT (NCTU)-NRT (ESA) is over DOY 345–347, 2011.

signs. Again, the differences for NCTU-UCAR and NCTU-ESA are large because they are based on NRT estimations and different clock references. The UCAR-CODE and NCTU-CODE differences are similar, and both the differences vary over different satellites. The differences in Fig. 5 are consistent with the statistics in Table I, but Fig. 5 shows the variations over satellites. We expect that our system will deliver a much improved GPS clock solution when the full set of available GPS ground stations is used.

IV. Determination and Assessment of NRT Orbit and Clock of LEO

As stated in Section I, our NRT OD follows the same procedure as that for the PP processing [24]. The reduced-dynamic approach with zero-differenced ionosphere-free GPS carrier phases is used for NRT OD. Our OD system detects the latest observations and generates 10-s COSMIC orbits every 10 min by the automatic procedure (see Fig. 1). For NRT operation, the LEO OD is typically performed over orbit arc lengths between 6 and 12 h. In this paper, the orbit arc length for OD was set to 6 h, in which the data are from the latest GPS session and the previous GPS session. As an example, Fig. 6 shows the lengths of GPS sessions from five COSMIC satellites (FM3 data are unavailable) over DOY 83–90, 2011. In total, there are 331 GPS sessions over this period. Compared to other satellites, FM1 and FM4 have less data gaps. The session lengths vary over different satellites, and the mean session length is 150 min (see Fig. 3).

Since COSMIC is not equipped with the SLR retroreflector, there is no external tracking data that can be used to validate the NRT orbit of COSMIC. Therefore, we assessed the accuracy of the NRT (NCTU) orbit by computing the following: 1) the differences between two overlapping NRT orbits (overlapping arc length: 100 min) and 2) the differences between the NRT and the PP orbits. The PP orbits in this paper were computed using the final GPS ephemeris, final Earth rotation parameters, and final GPS clocks at 30-s intervals from CODE and were
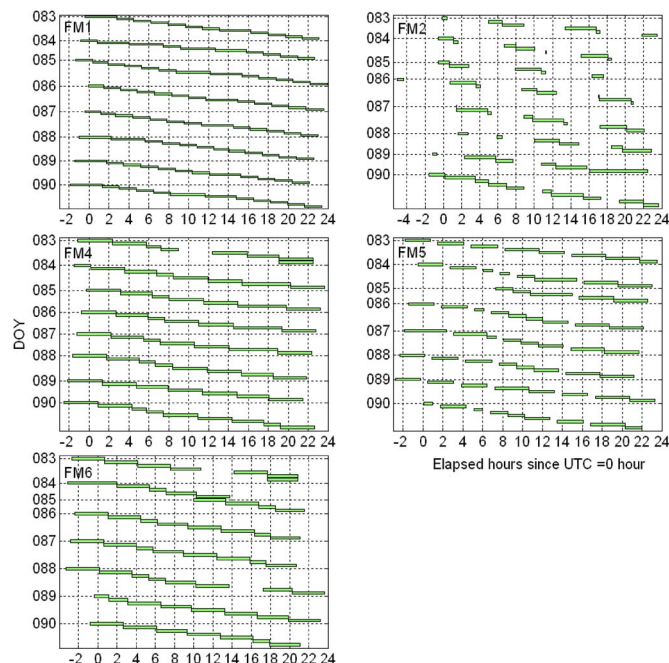

Fig. 6.　GPS session lengths (green bars) from FM1 to FM6 over DOY 83–90, 2011. For a DOY, the hour is counted from UTC of 0 h.

regarded as the reference (or true) orbits. A detailed description of the PP orbit is given by Hwang *et al.* [24], which show that, with proper data selection and processing, the mean accuracy of the PP orbits of the six COSMIC satellites can reach 2–3 cm. Furthermore, the OD procedure described in [24] also can be used to determine the kinematic orbits of COSMIC and Gravity Recovery and Climate Experiment (GRACE). The kinematic orbits of COSMIC have been used to compute the low-degree time-varying gravity field, which agrees with the SLR-derived result of 80% [31]. We also assessed the NRT (UCAR) orbit in the same manner. The NRT (UCAR) orbit is currently used in the operational applications of COSMIC data and is a product of both CDAAC and TACC.

Fig. 7 shows the orbit differences, and Table II shows the rms orbit differences in position and velocity for the cases in Fig. 7. Again, because there are no FM3 data during this period, FM3 is not included in the discussion. Fig. 7(a) shows the cases between two real-time orbits (NCTU-NCTU and UCAR-UCAR; only the differences in the overlapping arcs are counted), and Fig. 7(b) shows the cases between the real-time and PP orbits (the latter is produced by NCTU; see [24]). In the NRT (UCAR) solution, FM5 has a relatively large mean rms difference of 0.3 m (the mean is over eight days) as compared to other FMs. In comparison, the rms difference for FM5 from the NRT (NCTU) solution is 0.1 m. However, the difference for FM6 from the NRT (NCTU) solution is the largest among all FMs and is slightly larger than those from the NRT (UCAR) solution. Fig. 7 shows that the orbit accuracy of NRT (NCTU) is consistent with that of NRT (UCAR). Both the results in Fig. 7(a) and (b) indicate that the NRT (UCAR) solution for FM5 on DOY 88 results in a relatively large rms difference and, in turn, a relatively large orbit error. Fig. 7(c) shows the rms differences between the NRT (NCTU) and NRT (UCAR) orbits and the mean rms differences averaged over the five satellites.
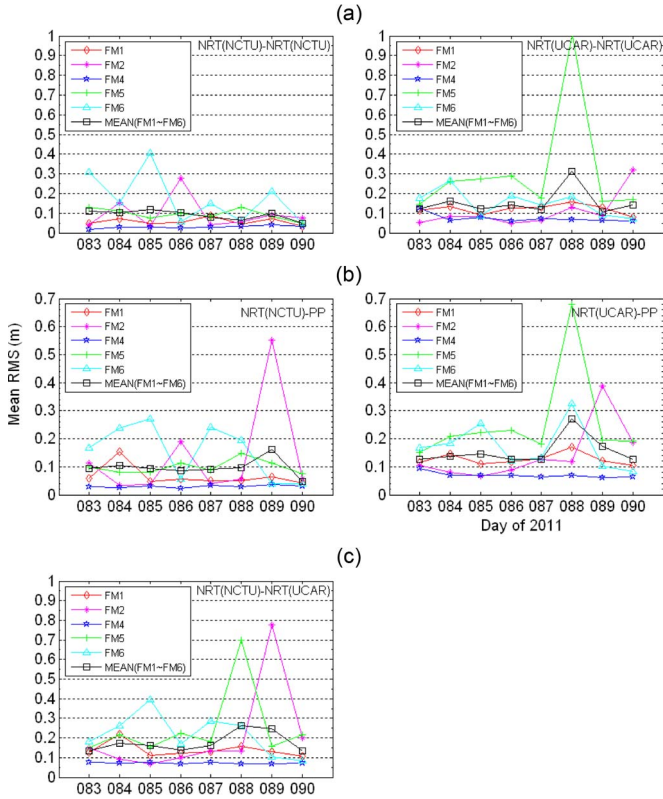
Fig. 7. Daily rms orbit differences over DOY 83–90, 2011 between (a) two self-NRT solutions, (b) NRT and PP solutions, and (c) two cross-NRT solutions.

TABLE II
RMS ORBIT DIFFERENCES (3-D) IN POSITION AND VELOCITY

Case of orbit difference	Position (m)	Velocity (mm/s)
[1]NRT (NCTU) – NRT (NCTU)	0.085/0.124/0.060[a]	0.204/0.315/0.194
[1]NRT (UCAR) – NRT (UCAR)	0.107/0.201/0.152	0.245/0.269/0.221
[1]NRT (NCTU) – PP	0.070/0.178/0.043	0.254/0.289/0.173
[1]NRT (UCAR) – PP	0.109/0.232/0.120	0.253/0.281/0.239
[1]NRT (NCTU) – NRT (UCAR)	0.151/0.239/0.141	0.291/0.298/0.195
[2]NRT (NCTU) – NRT (ESA)	0.061/0.101/0.080	0.091/0.094/0.088

[1] over five COSMIC satellites and over DOY 83–90, 2011
[2] for MetOp –A satellite and over DOY 345–347, 2011
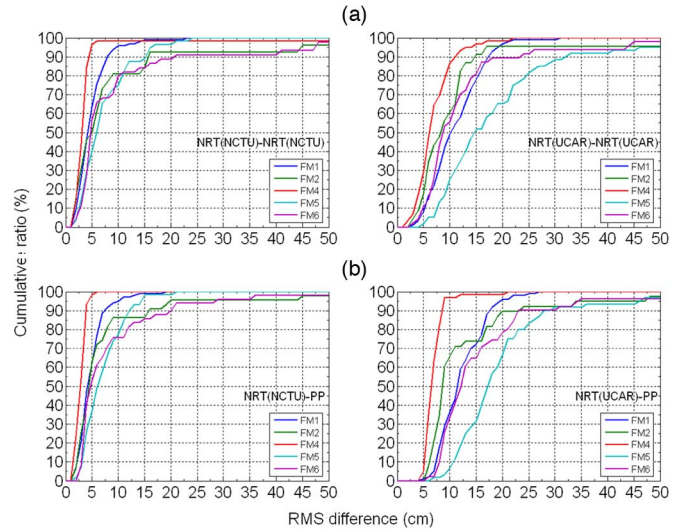[a] Radial/Along-track/Cross-track

Fig. 8. Cumulative ratios of orbit difference for (a) the NRT-NRT solutions and (b) the NRT and PP solutions, averaged over DOY 83–90, 2011 and five COSMIC satellites.

The difference varies from one satellite to another, and FM4 has the least difference (smaller than 0.1 m). The comparison in Fig. 7(c) confirms that the NRT (NCTU) orbit is qualified for the operational use of COSMIC and future COSMIC-2 because it performs equally well as the NRT (UCAR) orbit.

The differences in position and velocity in the case of NRT (NCTU)-NRT (NCTU) are 9 cm and 0.24 mm/s, respectively, which have the same level of accuracy as their counterparts (15 cm and 0.25 mm/s) in the case of NRT (UCAR)-NRT (UCAR). The comparisons between the NRT (both NCTU and UCAR)-PP solutions result in almost the same numbers as those in the NRT-NRT cases (e.g., 0.097 m versus 0.090 m for NCTU). The comparison between the NRT (NCTU) and the NRT (UCAR) solutions yields a 18-cm difference in position and a 0.26-mm/s difference in velocity, suggesting that the two NRT solutions are consistent at the decimeter level for position and the submillimeter-per-second level for velocity. In view of the different GPS clocks and different auxiliary data used in the NRT (NCTU) and the NRT (UCAR) solutions, the small discrepancies (at decimeter and submillimeter-per-second levels) in the two NRT orbits are remarkable. Although we did not carry out an external assessment of the NCTU OD system in this paper, there are some indirect assessments of this system. For example, Hwang *et al.* [24] compared the NCTU PP (postprocessed) orbit and the Wuhan PP orbit of COSMIC, the latter being determined by the OD software PANDA. Schreiner *et al.* [29] compared the UCAR PP orbit and the GFZ and JPL PP orbits of COSMIC. The NCTU-Wuhan orbit difference is at the 10-cm level, and the UCAR-GFZ and

the UCAR-JPL orbit difference are at 13.2- and 10.4-cm levels, respectively. These orbit differences are similar in magnitude to the orbit differences in Table II (ranging from 9 to 18 cm).

We also investigated the distributions of orbit errors. For this, we computed the cumulative ratios (in percentage) of the rms orbit differences from the 331 sessions given in Fig. 6. Fig. 8(a) shows the cumulative ratio as a function of rms orbit differences for the NRT orbits in Fig. 7(a). About 80% of the orbit differences from the NRT (NCTU) solution range from 0 to 10 cm. For example, about 98% of the orbit differences for FM4 are smaller than 10 cm (see the red curve in Fig. 8(a), left). In contrast, most of the orbit differences from the NRT (UCAR) solution range from 10 to 15 cm, except FM4. The two cases in Fig. 8(b) are similar to those in Fig. 7(b) but are for the cumulative ratios of the differences between the NRT and PP orbits. The patterns in Fig. 8(b) are similar to those in Fig. 8(a) in that the differences between the NRT (NCTU) and PP orbits are more concentrated at smaller values than the
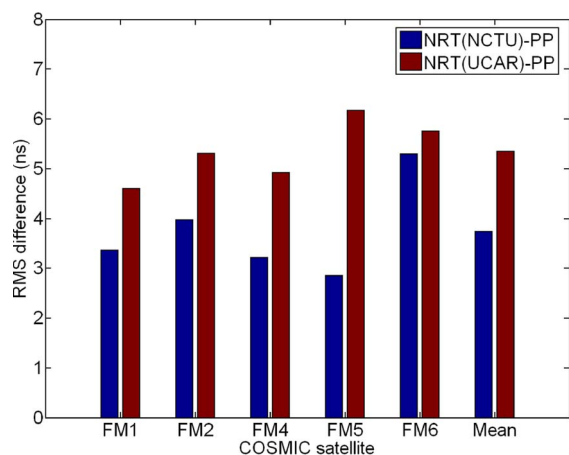
Fig. 9. RMS differences in estimated clock between the NRT (both NCTU and UCAR) and PP solutions for each COSMIC satellite, averaged over DOY 83–90, 2011.

Fig. 10. Geometry showing the single-differenced phase observations formed by the receiver r (on a COSMIC LEO), the occulted signal from GPS s to r, and the nonocculted signal from GPS p to r.

NRT (UCAR)-PP differences. Fig. 8 suggests that, in general, the NRT (NCTU) solution results in a smaller orbit error than the NRT (UCAR) solution. Most of the differences ($> 90\%$) between the NRT (UCAR) and the PP orbits are larger than 5 cm (see Fig. 8(b), right). In contrast, only about 40% of the differences between the NRT (NCTU) and the PP orbits are larger than 5 cm.

We also assessed the NRT COSMIC clocks estimated by the NRT NCTU and UCAR solutions against the PP solution. Fig. 9 shows the rms differences in COSMIC clock between the NRT and PP results. The rms differences in the cases of NRT (NCTU)-PP and NRT (UCAR)-PP are 3.742 and 5.352 ns, respectively, suggesting that the NRT (NCTU) solution yields a smaller error in COSMIC clock than the NRT (UCAR) solution. Again, the rms difference varies from one satellite to another, but the variation is smaller than 1 ns for both the NRT NCTU and UCAR solutions. In general, the orbit and clock estimates of LEO are correlated: A good LEO orbit solution implies a good LEO clock solution and vice versa. This statement is supported by the statistics in Table II and Figs. 7–9. For example, Table II shows that the NRT (NCTU) solution results in a smaller rms overlapping orbit difference, which is consistent with the smaller discrepancy of NCTU's COSMIC clock estimate against the PP result. As for the UCAR solution, the larger orbit difference (see Table II) coincides with the larger discrepancy of the clock solution (against the PP result; see Fig. 9). Note that the rms difference in COSMIC clock between the NRT (NCTU) and PP solutions is 3.742 ns (see Fig. 9), which is about two times larger than the rms difference of 1.427 ns in GPS clocks (see Table I). However, as will be demonstrated in Section V, the use of a single difference will reduce the impact of the LEO clock on the RO data retrieval, and instead, the GPS clocks will have a dominating effect on RO results.

As an independent verification of our OD system for satellite missions other than COSMIC, in Table II, we also compare orbits and velocities of the MetOp-A satellite from the NRT (NCTU) and the NRT (ESA) solutions over DOY 345–347, 2011. The MetOp mission is a joint EUMETSAT and ESA RO mission [11], [32]–[34], containing a series of three po-
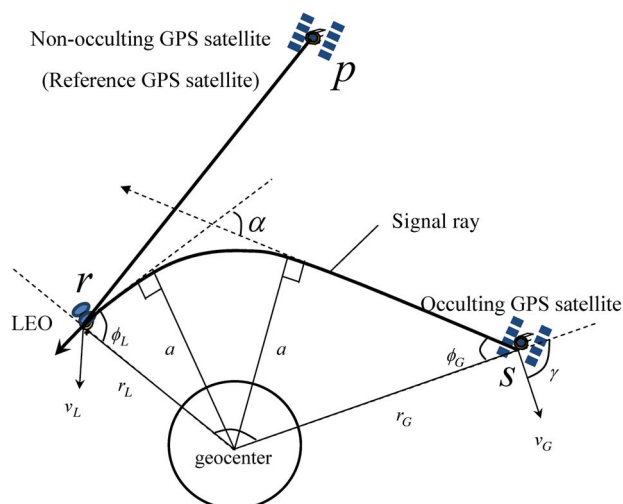
lar orbiting meteorological satellites operating for over 14 years. MetOp-A was launched on October 19, 2006, MetOp-B was launched on September 17, 2012, and MetOp-C will be launched in 2017. The NRT (ESA) orbits of MetOp-A are estimated by the NAPEOS software system in ESA. The orbits are determined by precise point positioning as in this paper but using the real-time GPS orbits and clocks from ESA. The 3-D rms position and velocity differences of MetOp-A in the case of NRT (NCTU)-NRT (ESA) over the three days are about 8 cm and 0.09 mm/s (see Table II), which are slightly worse but consistent with the interagency orbit comparisons presented in [34] and a one-month external orbit comparison given in [11]. Table II confirms the reliability of our OD system and suggests that the overall MetOp-A orbit quality is better than that of COSMIC. A degraded orbit accuracy of COSMIC with respect to MetOp-A is expected because of the inherent limitations of COSMIC's small spacecraft design and its problems in attitude determination and control system [25], [35], [36].

V. Analysis of Orbit and Clock Errors on Excess Phase, Doppler Shift, and Bending Angle

The atmospheric excess phase (relative to vacuum) is the phase delay between the GPS transmitter and the LEO receiver caused by the ionosphere and the neutral atmosphere, and it is the basic observable in an occultation event [8]. The main error sources in determining the excess phase are satellite orbits (both GPS satellite and LEO), measured traveling time between the transmitter and the receiver, GPS clock, and LEO frequency stability. The excess phase can be computed using either the double-difference, the single-difference (SD), or the zero-difference processing strategy [8], [9], [29], [37]–[39]. The SD processing strategy is used in CDAAC, both in the NRT and PP modes. CDAAC uses L1 and L2 carrier phase measurements, sampled at 50 Hz, to retrieve atmospheric profiles. Fig. 10 shows the geometry in the SD processing, where satellites s and p represent the occulting and the nonocculting GPS satellites,

respectively. In Fig. 10, r_G and r_L are the geocentric distances of the GPS satellites and LEO, v_G and v_L are their velocity vectors, ϕ_G and ϕ_L represent the angles between the directions of the transmitting/received signals and the directions to the geocenter, γ is the angle between r_G and v_G, a is the impact parameter, and α is the bending angle.

Without the phase ambiguity and noise, the observed carrier phase (L_r^s) between the receiver r on a LEO and the occulting GPS satellite s is

$$L_{r,i}^s = \rho_r^s + c \cdot \delta_r - c \cdot \delta^s + dI_{r,i}^s + dT_r^s \qquad (1)$$

where

i　　GPS signal frequency: $i = 1$ for L_1, and $i = 2$ for L_2;
ρ_r^s　geometric range between receiver r and GPS s;
c　　speed of light in vacuum;
δ_r　receiver clock error;
δ^s　GPS satellite clock error at signal emission time;
$dI_{r,i}^s$　ionospheric delay (frequency dependent with the sign included);
dT_r^s　tropospheric delay (frequency independent with the sign included).

In (1), the geometric distance is between the position of the receiver at reception time t and the satellite position at the transmission time, i.e., $t - \tau_r^s$, where τ_r^s is the signal traveling time. In order to eliminate the errors at the receiver, the SD phase at a LEO receiver between the phases to an occulting and a nonocculting GPS satellite is formed. The L_3 phase to p, $L_{r,3}^p$, is computed by the combination of L_1 and L_2 as [11]

$$L_{r,3}^p = L_{r,1}^p + c_2 \langle L_{r,1}^p - L_{r,2}^p \rangle = \rho_r^p + c \cdot \delta_r - c \cdot \delta^p + dT_r^p \qquad (2)$$

where $c_2 = f_2^2/(f_1^2 - f_2^2)$, $f_1 = 1575.42$ MHZ, and $f_2 = 1227.60$ MHZ; $\langle \rangle$ denotes smoothing with a 2-s window to reduce the L_2 noise [29], [39], [40]. The excess phase can be estimated by the SD phase resulting from (1) and (2)

$$EP_{r,i}^{s,p} = L_{r,i}^s - L_{r,3}^p - [\rho_r^s - \rho_r^p - c(\delta^s - \delta^p)] = dI_{r,i}^s + dT_r^s. \qquad (3)$$

In (3), the tropospheric effect dT_r^p can be set to zero because there is no such an effect from the LEO to the nonocculting GPS satellite, the range difference $(\rho_r^s - \rho_r^p)$ is computed from the GPS satellite and LEO orbits (see Section IV), and $(\delta^s - \delta^p)$ is computed from the estimated GPS clocks (see Section III). As a result, the differenced phase in (3) contains no LEO clock and can be used to estimate the excess phase due to the ionosphere and troposphere.

The Doppler shift is the frequency difference between the received signal and the source signal due to the relative motion between the platforms hosting the two signals. The time derivative of the excess phase will add to the Doppler shift, resulting in the excess Doppler shift as

$$\frac{dEP_{r,i}^{s,p}}{dt} = \dot{L}_{r,i}^s - \dot{L}_{r,3}^p - \left[\dot{\rho}_r^s - \dot{\rho}_r^p - c(\dot{\delta}^s - \dot{\delta}^p) \right] = d\dot{I}_r^s + d\dot{T}_r^s \qquad (4)$$

where a dot over a variable represents its first derivative with respect to time. The excess Doppler shift can be used to derive

TABLE III
STATISTICS OF THE DIFFERENCES IN L_1 EXCESS PHASE
(IN CENTIMETERS) AND L_1 EXCESS DOPPLER SHIFT
(IN MICROMETERS PER SECOND) BETWEEN
NRT AND PP SOLUTIONS

Case	Excess Phase			Excess Doppler shift		
	RMS	Std Dev	Mean	RMS	Std Dev	Mean
NRT (NCTU) – PP	4.045	2.038	3.494	26.965	16.533	21.302
NRT (UCAR) – PP	3.625	1.864	3.109	23.468	13.804	18.979

the bending angle, refractivity, geopotential height, pressure, temperature, and humidity along occulting profiles. Here, we assess the excess phase and excess Doppler shift derived from the NRT (NCTU) and NRT (UCAR) products against the PP product. A product here includes the COSMIC orbits, COSMIC clocks, and GPS clocks. Like the assessments made in Sections III and IV, the excess phase and excess Doppler shift derived from the PP are regarded as the "true" or "standard" value. Again, the selected data cover DOY 83–90, 2011, during which 12 393 RO observable files exist. Table III summarizes the statistics of the differences in the excess phases and excess Doppler shift between the NRT and PP results. Table III is to illustrate the effect of using different orbit products on the excess phase and excess Doppler shift. Typically, the noises of the observed L_1 and L_2 phases will cause deviations of the assumption of spherical symmetry in an inversion algorithm of bending angle. Such a deviation is especially large when using L_2 observations [11], [29], [41]. Because we want to focus on the impact of the LEO orbit and clock on RO results, we choose to use only L_1 observations to demonstrate this impact in Table III. For a practical RO parameter retrieval, excess phases and Doppler shifts will be filtered and combined to yield an optimal result. The differences in the NRT (NCTU)-PP case are larger than those in the NRT (UCAR)-PP case. The reasons are as follows: 1) The GPS clock remains effective in the SD-derived excess phase and Doppler shift, and 2) the NRT (NCTU) solution shows larger differences in GPS clock with the PP solution (see Table I) than the NRT (UCAR) solution due to the use of a partial GPS ground network in the NRT (NCTU) solution.

To quantify the effect of GPS clock error on bending angle, we computed the GPS frequency stability from the estimated high-rate GPS clocks in Section III (see also Table I). The frequency stability is a measure of the divergence of the estimated clocks. In the GPS literature, the Allan deviation [42] of estimated clocks is regarded as the frequency stability. A numerical example of frequency stability estimation for two ground GPS receivers in Taiwan is given by Yeh et al. [43], [44]. Using the definition of the Allan deviation [42], the frequency stabilities based on the estimated GPS clocks (see Section III) from the NRT (NCTU) and NRT (UCAR) solutions over DOY 83–90, 2011 (at 30-s intervals) are 6.1E-12 and 2.7E-12, respectively. These instabilities can cause clock-induced range fluctuations of 5.5 and 2.4 cm. In comparison, the frequency stability from

the final IGS product (at 30-s sampling intervals of clock) is about 2E-12 and causes a clock-induced range fluctuation of 2 cm [29], [45].

The error in bending angle caused by GPS frequency stability can be approximated by [46]

$$\delta\alpha_f = \frac{r_G c \cos\phi_G}{r_L v_G \cos(\pi - \phi_L) \sin(\gamma - \phi_G)}\delta f \qquad (5)$$

where δf is the frequency stability and the definitions of other variables are given in Fig. 10. As a numerical example, the mean bending angle errors caused by the GPS frequency insta-bilities for all RO signals received by FM1 on DOY 90, 2011 from the NRT (NCTU), NRT (UCAR), and final IGS solutions are 3.75, 1.66, and 1.23 μrad, respectively. In this case, the GPS clock-induced error from the NRT (NCTU) solution is about 2 times larger than that from the NRT (UCAR) solution. Compared to the altitudes below 60 km, which is the maximum altitude of the atmospheric profiles provided with CDAAC, the effects of the ionosphere and troposphere at the altitudes of 60–80 km on the bending angle are insignificant [11], [29], [41]. Therefore, we choose altitudes of 60–80 km to assess the impact of POD on the bending angle to minimize other effects. Considering the random error of 1.5 μrad in the bending angle caused by disturbance in the neutral atmosphere at 60–80 km [29], the GPS-induced bending angle error from the NRT (UCAR) solution (1.66 μrad) is nearly acceptable for the need of RO data retrieval. However, the GPS-induced bending angle error from the NRT (NCTU) solution (3.75 μrad) is still too large to be used for RO data retrieval. This analysis highlights the need of the NRT (NCTU) system to improve its GPS ground network for an improved GPS clock solution.

We also assessed the bending angle error caused by the LEO velocity error using the approximate formula [29]

$$\delta\alpha_v \approx \frac{\delta v}{v_L \tan\phi_L} \qquad (6)$$

where δv is the LEO velocity error (see Fig. 10 for other variables in this equation). By the error propagation rule in case of no correlation between the involving variables, the velocity differences in Table II can be used to infer the orbit velocity error using the simple approximation that velocity error equals velocity difference divided by $\sqrt{2}$. For example, the velocity error from the NRT (NCTU) orbit is $0.238/\sqrt{2} = 0.168$ mm/s. Fig. 11 shows the bending angle error for a LEO velocity error of 0.1 mm/s at the LEO velocity = 7 km/s. As a numerical example, if $v_L \sim 7$ km/s, $\delta v \sim 0.168$ mm/s, and $\phi_L \sim 25°$, the bending angle error is 0.051 μrad($= 0.168/7/\tan 25°$), which is also equal to 1.68($= 0.168/0.1$) times the value of the bending angle error at $\phi_L = 25°$ in Fig. 11. This error (0.051 μrad) is considerably smaller than the 1.5-μrad random noise of neutral atmospheric bending angles between 60 and 80 km [29]. From the result in Table II, both the LEO orbits from the NRT (NCTU) and NRT (UCAR) solutions are quali-fied for the RO data retrieval.
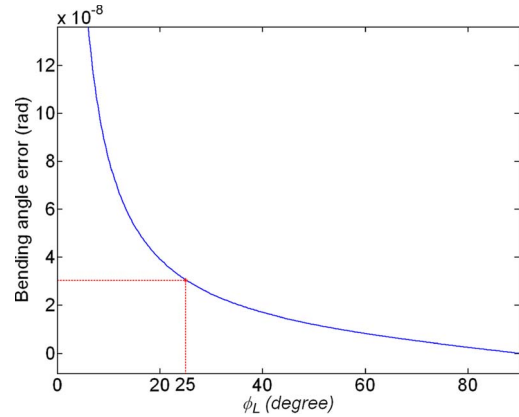

Fig. 11. The bending angle error as a function of ϕ_L for a LEO velocity error = 0.1 mm/s.

VI. CONCLUSION

For the first time in Taiwan, we have developed an automatic system under Linux/PC, called the NRT (NCTU) system, which is capable of determinations of the NRT high-rate GPS clock and LEO orbit and clock. This system is expected to be part of the RO processing system in NSPO for future COSMIC-2 mission. The current NRT (NCTU) system has limitations in accessing ground GPS data and in efficient data flow, but such limitations will be removed once it becomes a part of the core system that does the routine processing of real-time COSMIC or COSMIC-2 data. Verifications of the system are made using COSMIC data. Compared to the NRT (UCAR) system, the COSMIC orbits and clocks from the NRT (NCTU) system have smaller discrepancy with the PP result. The COSMIC orbit accuracy from the NRT (NCTU) system is about 10 cm, and the system provides consistent OD results as NRT (UCAR). For the COSMIC data used in this paper, the mean orbit error from the NRT (NCTU) system results in a velocity error of 0.168 mm/s, which contributes a 0.051 μrad error to the bending angle. In view of the atmospheric disturbance in GPS phase measurements, this orbit-induced error in bending angle is negligible, and the NRT (NCTU) system is qualified for RO data retrieval.

For an automatic NRT OD system, computational efficiency is also an important issue. We improve the efficiency of the time-consuming GPS clock estimation by 64% using a par-allel scheduling. The frequency stability from the GPS clock determined from the NRT (NCTU) system is about 6.1E-12, corresponding to a range fluctuation of 5.5 cm and contributing a 3.75-μrad error to the bending angle. The GPS-induced bending angle error from the NRT (NCTU) system is too large to be used for RO data retrieval, suggesting the need of the NRT (NCTU) system to improve its GPS ground network. This can be achieved once the NRT (NCTU) system is installed in the data processing centers for the COSMIC and COSMIC-2 missions.

The core processing software in our system is the Bernese GPS Software Version 5.0, which currently can process both GPS and GLONASS signals. A future software version will add the capability to process the Galileo signal. Our OD system will use a new release of the Bernese GNSS Software to process signals from a triple-constellation GPS/GLO/GAL receiver.

REFERENCES

[1] C. J. Fong, D. Whiteley, E. Yang, K. Cook, V. Chu, B. Schreiner, D. Ector, P. Wilczynski, T. Y. Liu, and N. Yen, "Space and ground segment performance and lessons learned of the FORMOSAT-3/COSMIC mission: Four years in orbit," *Atmos. Meas. Technol.*, vol. 4, no. 6, pp. 1115–1132, Jun. 2011.

[2] Y. A. Liou, A. G. Pavelyev, S. F. Liu, A. A. Pavelyev, N. Yen, C. Y. Huang, and C. J. Fong, "FORMOSAT-3/COSMIC GPS radio occultation mission: Preliminary results," *IEEE Trans. Geosci. Remote Sens.*, vol. 45, no. 11, pp. 3813–3826, Nov. 2007.

[3] J. Wickert, T. Schmidt, G. Michalak, S. Heise, C. Arras, G. Beyerle, C. Falck, R. König, and D. Pingel, "GPS radio occultation with CHAMP and GRACE-A, SAC-C, TerraSAR-X, and FORMOSAT-3/COSMIC: Brief review of results from GFZ," in *New Horizons in Occultation Research, Studies in Atmosphere and Climate*, A. Steiner, B. Pirscher, U. Foelsche, and G. Kirchengast, Eds. Berlin/Heidelberg, Germany: Springer-Verlag, 2009.

[4] T. K. Meehan, "The TriG digital beam steered sounder," in *Proc. IEEE Conf. Aerosp.*, 2009, pp. 1–5.

[5] S. Jin, G. P. Feng, and S. Gleason, "Remote sensing using GNSS signals: Current status and future directions," *Adv. Space Res.*, vol. 47, no. 10, pp. 1645–1653, May 2011.

[6] C. Urschl, G. Beutler, W. Gurtner, U. Hugentobler, and S. Schaer, "Contribution of SLR tracking data to GNSS orbit determination," *Adv. Space Res.*, vol. 39, no. 10, pp. 1515–1523, 2007.

[7] D. Svehla and M. Rothacher, "Kinematic and reduced-dynamic precise orbit determination of low Earth orbiters," *Adv. Geosci.*, vol. 1, pp. 47–56, Jun. 2003.

[8] E. R. Kursinski, G. A. Hajj, J. T. Schofield, R. P. Linfield, and K. R. Hardy, "Observing Earth's atmosphere with radio occultation measurements using the Global Positioning System," *J. Geophys. Res.*, vol. 102, no. D19, pp. 23 429–23 466, Oct. 1997.

[9] G. A. Hajj, E. R. Kursinski, L. J. Romans, W. I. Bertiger, and S. S. Leroy, "A technical description of atmospheric sounding by GPS occultation," *J. Atmos. Sol. Terr. Phys.*, vol. 64, no. 4, pp. 451–469, Mar. 2002.

[10] H. Anlauf, D. Pingel, and A. Rhodin, "Assimilation of GPS radio occultation data at DWD," *Atmos. Meas. Tech.*, vol. 4, no. 2, pp. 1533–1554, Mar. 2011.

[11] W. Schreiner, S. Sokolovskiy, D. Hunt, C. Rocken, and Y. H. Kao, "Analysis of GPS radio occultation data from the FORMOSAT-3/COSMIC and Metop/GRAS missions at CDAAC," *Atmos. Meas. Tech.*, vol. 4, no. 10, pp. 2255–2272, Oct. 2011.

[12] R. A. Anthes, P. A. Bernhardt, Y. Chen, L. Cucurull, K. F. Dymond, D. Ector, S. B. Healy, S.-P. Ho, D. C. Hunt, Y.-H. Kuo, H. Liu, K. Manning, C. McCormick, T. K. Meehan, W. J. Randel, C. Rocken, W. S. Schreiner, S. V. Sokolovskiy, S. Syndergaard, D. C. Thompson, K. E. Trenberth, T.-K. Wee, N. L. Yen, and Z. Zeng, "The COSMIC/ FORMOSAT-3 mission: Early results," *Bull. Amer. Meteorol. Soc.*, vol. 89, no. 3, pp. 313–333, Mar. 2008.

[13] Y. Bar-Sever, B. Bell, A. Dorsey, and J. Srinivasan, "Space applications of the NASA global differential GPS system," Institute of Navigation, Portland, OR, USA, 2003.

[14] J. Pérez, L. Agrotis, and J. Fernández, "ESA/ESOC real time data processing," in *Proc. IGS Workshop*, Darmstadt, Germany, 2006, pp. 1–11.

[15] A. Hauschild and O. Montenbruck, "Kalman-filter-based GPS clock estimation for near real-time positioning," *GPS Solution*, vol. 13, no. 3, pp. 173–182, Jul. 2009.

[16] M. Caissy, G. Weber, L. Agrotis, G. Wübbena, and M. Hernandez-Pajares, "The IGS real-time pilot project—The development of real-time IGS correction products for precise point positioning," presented at the Proc. EGU, Vienna, Austria, Apr. 6, 2011.

[17] H. Li, J. Chen, J. Wang, C. Hu, and Z. Liu, "Network based real-time precise point positioning," *Adv. Space Res.*, vol. 46, no. 9, pp. 1218–1224, Nov. 2010.

[18] M. Ge, J. Chen, and G. Gendt, "EPOS-RT: Software for realtime GNSS data processing. Geophysical research abstracts," in *Proc. EGU Gen. Assembly*, Vienna, Austria, 2009, vol. 11, p. EGU2009-8933.

[19] M. Ge, J. Chen, and J. Dousa, "A computationally efficient approach for estimating high-rate satellite clock corrections in realtime," *GPS Solutions*, vol. 16, no. 1, pp. 9–17, Jan. 2012.

[20] R. Dach, U. Hugentobler, P. Fridez, and M. Meindl, *Bernese GPS Software—Version 5.0. Astronomical Institute.* Bern, Switzerland: Univ. of Bern, 2007.

[21] R. Dach, E. Brockmann, S. Schaer, G. Beutler, M. Meindl, L. Prange, H. Bock, A. Jäggi, and L. Ostini, "GNSS processing at CODE: Status report," *J. Geod.*, vol. 83, no. 3/4, pp. 353–366, Mar. 2009.

[22] Y. Mitsui and K. Heki, "Observation of Earth's free oscillation by dense GPS array: After the 2011 Tohoku megathrust earthquake," *Sci. Commun.*, vol. 2, p. 931, Dec. 2012.

[23] H. Bock, R. Dach, A. Jäggi, and G. Beutler, "High-rate GPS clock correction from CODE: Support of 1 Hz applications," *J. Geod.*, vol. 83, no. 11, pp. 1083–1094, Nov. 2009.

[24] C. Hwang, T. P. Tseng, T. Lin, D. Švehla, and B. Schreiner, "Precise orbit determination for the FORMOSAT-3/COSMIC satellite mission GPS," *J. Geod.*, vol. 83, no. 5, pp. 477–489, May 2009.

[25] T. P. Tseng, C. Hwang, and S. K. Yang, "Assessing attitude error of FORMOSA-3/COSMIC satellites and its impact on orbit determination," *Adv. Space Res.*, vol. 49, no. 9, pp. 1301–1312, May 2012.

[26] J. Wickert, G. Michalak1, T. Schmidt, G. Beyerle, C. Z. Cheng, S. B. Healy, S. Heise1, C. Y. Huang, N. Jakowski, W. Köhler, C. Mayer, D. Offiler, E. Ozawa, A. G. Pavelyev, M. Rothacher, B. Tapley, and C. Arras, "GPS radio occultation: Results from CHAMP, GRACE and FORMOSAT-3/COSMIC," *Terr. Atmos. Ocean. Sci.*, vol. 20, no. 1, pp. 35–50, Feb. 2009.

[27] G. Michalak and R. Konig, "Near-real time satellite orbit determination for GPS radio occultation with CHAMP and GRACE," in *System Earth via Geodetic-Geophysical Space Techniques*, F. Flechtner, T. Gruber, A. Guntner, M. Mandea, M. Rothacher, T. Schone, and J. Wickert, Eds. Berlin, Germany: Springer-Verlag, 2010, pp. 443–454.

[28] H. Bock, R. Dach, Y. Yoon, and O. Montenbruck, "GPS clock correction estimation for near real-time orbit determination applications," *Aerosp. Sci. Technol.*, vol. 13, no. 7, pp. 415–422, Oct./Nov. 2009.

[29] W. Schreiner, C. Rocken, S. Sokolovskiy, and D. Hunt, "Quality assessment of COSMIC/FORMOSAT-3 GPS radio occultation data derived from single- and double-difference atmospheric excess phase processing," *GPS Solution*, vol. 14, no. 1, pp. 13–22, Jan. 2010.

[30] A. Agueda and R. Zandbergen, "NAPEOS Mathematical Models and Algorithms," ESA/ESOC, Darmstadt, Germany, NAPEOS-MM-01, 2004, 3.0.

[31] T. Lin, C. Hwang, T. P. Tseng, and B. F. Chao, "Low-degree gravity change from GPS data of COSMIC and GRACE satellite missions," *J. Geodyn.*, vol. 53, pp. 34–42, Jan. 2012.

[32] M. Cohen, G. Mason, Y. Buhler, D. Provost, D. Klaes, X. Calbet, and E. Oriol-Pibernat, "The EUMETSAT Polar System," ESA Bull., Paris, France, 127, pp. 19–23, 2006.

[33] K. D. Klaes and M. Cohen, "An introduction to the EUMETSAT polar system," *Bull. Amer. Meteorol. Soc.*, vol. 88, no. 7, pp. 1085–1096, Jul. 2007.

[34] O. Montenbruck, Y. Andres, H. Bock, T. van Helleputte, J. van den Ijssel, M. Loiselet, C. Marquardt, P. Silvestrin, P. Visser, and Y. Yoon, "Tracking and orbit determination performance of the GRAS instrument on MetOp-A," *GPS Solution*, vol. 12, no. 4, pp. 289–299, Sep. 2008.

[35] T. P. Tseng, K. Zhang, C. Hwang, U. Hugentobler, C. S. Wang, S. Choy, and Y. S. Li, "Assessing antenna field of view and receiver clocks of COSMIC and GRACE satellites: Lesson for COSMIC-2," *GPS Solution*, to be published.

[36] C. J. Fong, S. K. Yang, C. H. Chu, C. Y. Huang, J. J. Yeh, C. T. Lin, T. C. Kuo, T. Y. Liu, N. L. Yen, S. S. Chen, Y. H. Kuo, Y. A. Liou, and S. Chi, "FORMOSAT-3/COSMIC constellation spacecraft system performance: After one year in orbit," *IEEE Trans. Geosci. Remote Sens.*, vol. 46, no. 11, pp. 3380–3394, Nov. 2008.

[37] J. Wickert, G. Beyerle, G. A. Hajj, V. Schwieger, and C. Reigber, "GPS radio occultation with CHAMP: Atmospheric profiling utilizing the space-based single difference technique," *Geophys. Res. Lett.*, vol. 29, no. 8, pp. 28-1–28-4, Apr. 2002.

[38] J. Wickert, G. Beyerle, R. König, S. Heise, L. Grunwaldt, G. Michalak, C. Reigber, and T. Schmidt, "GPS radio occultation with CHAMP and GRACE: A first look at a new and promising satellite configuration for global atmospheric sounding," *Ann. Geophys.*, vol. 23, no. 3, pp. 653–658, Mar. 2005.

[39] G. Beyerle, T. Schmidt, G. Michalak, S. Heise, J. Wickert, and C. Reigber, "GPS radio occultation with GRACE: Atmospheric profiling utilizing the zero difference technique," *Geophys. Res. Lett.*, vol. 32, no. 13, pp. L13806-1–L13806-5, Jul. 2005.

[40] C. Rocken, R. Anthes, M. Exner, D. Hunt, S. Sokolovskiy, R. Ware, M. Gorbunov, W. Schreiner, D. Feng, B. Herman, Y. H. Kuo, and X. Zou, "Analysis and validation of GPS/MET data in the neutral atmosphere," *J. Geophys. Res.*, vol. 102, no. D25, pp. 29 849–29 860, Dec. 1997.

[41] S. Sokolovskiy, W. Schreiner, C. Rocken, and D. Hunt, "Optimal noise filtering for the ionospheric correction of GPS radio occultation signals," *J. Atmos. Ocean. Technol.*, vol. 26, no. 7, pp. 1398–1403, Jul. 2008.

[42] D. Allan and M. Weiss, "Accurate time and frequency transfer during common-view of a GPS satellite," in *Proc. Freq. Control Symp*, 1980, pp. 334–356.

[43] T. K. Yeh, C. Hwang, G. Xu, C. S. Wang, and C. C. Lee, "Determination of Global Positioning System (GPS) receiver clock errors: Impact on positioning accuracy," *Meas. Sci. Technol.*, vol. 20, no. 7, pp. 075105-1–075105-7, Jul. 2009.

[44] T. K. Yeh, C. H. Chen, G. Xu, C. S. Wang, and K. H. Chen, "The impact on the positioning accuracy of the frequency reference of a GPS receiver," *Surv. Geophys.*, vol. 34, no. 1, pp. 73–87, Jan. 2013.

[45] K. L. Senior, J. R. Ray, and R. L. Beard, "Characterization of periodic variation in GPS satellite clocks," *GPS Solution*, vol. 12, no. 3, pp. 211–225, Jul. 2008.

[46] S. V. Sokolovskiy, C. Rocken, and A. R. Lowry, "Use of GPS for estimation of bending angles of radio waves at low elevations," *Radio Sci.*, vol. 36, no. 3, pp. 473–480, May/Jun. 2001.

Tzu-Pang Tseng received the M.S. and Ph.D. degrees from the National Chiao-Tung University, Hsinchu, Taiwan, in 2006 and 2010, respectively.

He is currently an Assistant Research Fellow with the GPS Science and Application Research Center, National Central University, Zhongli City, Taiwan. His expertise focuses on precise orbit determination of low Earth orbiters, such as the FORMOSAT-3/Constellation Observing System for Meteorology, Ionosphere, and Climate (COSMIC) and GRACE satellites. Currently, his research activity focuses on the precise orbit determination-related calibration of the upcoming FORMOSAT-7/COSMIC-2 satellite using GNSS data.

Yi-Shan Li received the B.S. degree from the Chung Cheng Institute of Technology, National Defense University, Tauyuan, Taiwan, in 2000 and the M.S. degree from National Chiao Tung University, Hsinchu, Taiwan, in 2004, where she is currently working toward the Ph.D. degree. Her research focuses on precise orbit determination (POD) of low-Earth-orbiter satellites and GPS data processing.

Currently, she is developing a real-time automatic POD system for FORMOSAT-3/Constellation Observing System for Meteorology, Ionosphere, and Climate (COSMIC) and FORMOSAT-7/COSMIC-2 satellite missions.

Cheng-Yung Huang received the Ph.D. degree from the Institute of Space Science, National Central University, Jhongli, Taiwan, in 2005.

He is an Assistant Research Fellow with the GPS Science and Application Research Center, National Central University. He is working on the radio occultation (RO) technique for retrieving atmospheric profiles from RO and starts to study and develop the software for GNSS-R data process and application.

Cheinway Hwang received the M.S. and Ph.D. degrees in geodetic science from The Ohio State University, Columbus, OH, USA, in 1989 and 1991, respectively.

He was a Postdoctoral Research Associate in the Department of Earth Sciences, Oxford University, Oxford, U.K., in 1991–1993. He is currently a Chair Professor with the Department of Civil Engineering, National Chiao Tung University, Hsinchu, Taiwan. His major research areas are satellite geodesy and gravimetry.

Dr. Hwang was the recipient of the Distinguished Research Awards of the National Science Council of Taiwan in 1998, 2000, and 2002. He is a Fellow of the International Association of Geodesy.

Heike Bock received the diploma degree in geodesy from the Technical University of Karlsruhe, Karlsruhe, Germany, in 1998 and the Ph.D. degree in satellite geodesy from the Astronomical Institute of the University in Bern (AIUB), Bern, Switzerland, in 2003.

As a Senior Researcher at AIUB, she works in the field of precise orbit determination for low-Earth-orbiter satellites using GPS, and she has developed efficient procedures for GPS clock determination for postprocessing and near-real-time applications. In this position, she is also responsible for the operational precise orbit determination of the GOCE satellite.